

FTIR SPECTROSCOPIC STUDY ON BENIGN AND CANCEROUS HUMAN BREAST TISSUES - A RUN CHART ANALYSIS

G. Devi¹, T.S. Renuga Devi*² and S. Gunasekaran³

¹Department of Physics, R.M.K. College of Engineering and Technology, Pudukottai

² PG Department of Physics, Women's Christian College, Chennai

³Registrar, Periyar University, Salem

*E-mail: devi_renuga@yahoo.com, devinivash@gmail.com

ABSTRACT

Breast cancer tissues have been analyzed to determine the feasibility of the chemical changes taking place in the biological tissue, which can be identified and categorized into various grades. FTIR spectroscopy can be used for qualitative analysis of cancerous breast tissues because of its sensitivity to the changes in the biomolecules in the tissues. IR spectra was taken for a total number of 43 samples of human breast tissues which were already identified as normal, hyperplasia, fibro adenoma, ductal carcinoma and invasive ductal carcinoma breast tissues. The infrared spectrum was recorded in the frequency range between 400 cm⁻¹ and 1100 cm⁻¹. Some remarkable spectral differences were observed among normal, hyperplasia, fibro adenoma, ductal carcinoma and invasive ductal carcinoma tissues. The absorption bands were found to be at 538 cm⁻¹, 853 cm⁻¹, 935 cm⁻¹, 1005 cm⁻¹, 1080 cm⁻¹ were found to be the characteristic peaks which differentiate the benign tissues and cancerous breast tissues. The ratios $A_{538/853}$, $A_{538/935}$, $A_{538/1005}$, $A_{538/1080}$, $A_{853/935}$, $A_{853/1005}$, $A_{853/1080}$, $A_{935/1005}$, $A_{935/1080}$, $A_{1005/1080}$ were also determined and discussed. Thus it implies that FTIR spectroscopy is useful for the qualitative investigation of cancerous breast tissues.

Keywords: FTIR Spectroscopy, Breast cancer, Run chart analysis

INTRODUCTION

The breast cancer is the most common malignant tumor in women and the second major cause for death^{1, 2}. The breast undergoes many changes throughout a woman's life, both progressive due to puberty, pregnancy, menstruation and menopause. This dynamical activity could induce a lot of opportunities for disease. Breast pathology is divided into two main categories, benign and malignant pathologies³. The increased cell proliferation and metabolic activity in malignant tissue results in changes in the oxidation states of several biochemical species. Using the sensitivity of FTIR spectroscopy to the biomolecular changes in the tissues, many works⁴⁻⁸ has been done in the analysis of breast cancer tissues. The present work is focused on the variations in the collagen content in breast cancerous tissues which changes the spectral character accordingly during the carcinogenesis process. This spectral difference for the various carcinogenesis processes is studied using fitting line plot statistical method.

MATERIALS AND METHODS

Human breast tissues were obtained from pathology department at Government General Hospital, Madras Medical College, and Chennai. Each sample was cut into two pieces. The first one was sent to the pathologists for evaluation using their histopathological techniques. The second was frozen in saline water immediately after collecting it and used for IR spectroscopic recording within few hours. For FTIR spectroscopic recording the frozen tissues was taken as thin layer and dried then placed on the BaF₂ window in the spectrophotometer. Totally about 43 samples were collected. Among those 43

samples 10 were diagnosed as infiltrating ductal carcinoma, 10 as ductal carcinoma, 9 as fibro adenoma, 9 as hyperplasia and 5 as normal breast tissues.

Apparatus Description

The IR spectroscopy is carried out by using FT technique in PERKIN ELMER SPECTRUM ONE FTIR. IR spectroscopy involves the study of interaction of electromagnetic radiation with matter. Due to this interaction, electromagnetic radiation characteristic of the interacting system may be absorbed or emitted. The experimental data consists of the frequency and the intensity of the characteristic radiation absorbed or emitted.

The interference pattern from a two beam interferometer as the path difference between the two beams is altered, when Fourier transformed, gives rise to the spectrum. The transformation of the interferogram into spectrum is carried out mathematically with a dedicated on – line computer. The Perkin Elmer Spectrum One FTIR consists of Nerst glower as source, an interferometer chamber comprising of KB beam splitter followed by a sample chamber and detector. This instrument cover entire region of 4000 – 450 cm⁻¹. The spectrometer works under purged conditions.

Analysis

FTIR measures the changes in the cell status in the biomolecular structure and contents. The breast pathological tissues are mainly composed of collagen;⁹ proline, valine, glycine and phenylamine are the main collagen's amino acids. It is composed of both an epithelial component and a substantial stroma neoplastic element with collagen deposition.¹⁰ The spectrum of breast

tissues can be considered to be mainly from the overlapping of the epithelial cells and collagen in the connective tissue. The infrared spectra of the breast tissue in the frequency region 400 cm^{-1} and 1100 cm^{-1} are focused here. Proteins, nucleic acids, lipids and carbohydrates are the characteristic functional biomolecules in tissues. The change of the cell from normal status to malignant status induces changes in the relative content of the biomolecules.¹¹ The spectrum of breast tissues can be considered to be mainly from the overlapping of the epithelial cells and collagen in the connective tissue.

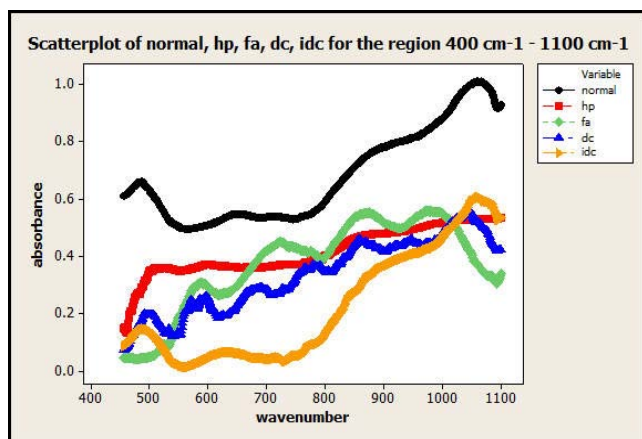


Figure 1: Scatter plot of normal, hyperplasia, fibroadenoma, ductal carcinoma, invasive ductal carcinoma.

The scatter plot of normal, hyperplasia, fibroadenoma, ductal carcinoma and invasive ductal carcinoma is shown in figure-1. The figure clearly differentiates benign and malignant breast tissues. The absorbance peak at 538 cm^{-1} is related to the disulphide bridges in cysteine corresponding to the s-s vibrational mode. The absorbance value at this peak is more for benign compared to malignant stages of breast cancer tissues. It was found that the lysosomal cysteine proteases cathepsin B and cathepsin L have been implicated in tumor spread and metastasis which is a underlining factor for tumor associated proteolysis for invasion and metastasis. In this

way the absorbance variation of the FTIR band at 538 cm^{-1} in normal tissue, hyperplasia, fibroadenoma, ductal carcinoma and invasive ductal carcinoma could be well understood when keeping this in mind these changes in cysteine content occurring in tumoral process.¹²

The absorbance peak at 853 cm^{-1} is the next significant FTIR band to be noted in the spectra. It was found that the absorbance is more for benign tissues less for cancerous tissues. The absorbance at this peak is due to the vibrational modes of (C-C) bond and (O-P-O) bond due to the presence of proline, tyrosine and DNA. Figure-1 also represents that at the peak near 935 cm^{-1} , the absorbance values of malignant have a higher value compared to benign stages of cancerous tissues. The absorbance here is due to the (C-C) bonding and α – helix bonding due to the presence of proline, valine, protein and glycogen.¹³ The absorbance peak at 1005 cm^{-1} is due to the symmetric ring vibrational mode due to the presence of phenylalanine. The absorbance is found to be higher for benign tissues compared to cancerous tissues. The peak at 1080 cm^{-1} is related to the (C-C), (C-O), (PO₂), (C-N), (O-P-O) vibrational modes. It represents the presence of nucleic acids, proteins and carbohydrates.

Comparative analysis among various breast cancer grades using Run Chart Analysis method.

The statistical method used for the IR spectroscopic analysis of human breast tissues for the region 400 cm^{-1} – 1100 cm^{-1} is the Run Chart Analysis. Variation occurs in all processes. Common cause variation is a natural part of the process. Another type of variation called the special causes comes from outside the system and causes recognizable patterns, shifts or trends in the absorbance data. The run chart shows if special causes are influencing the change in the process. Run chart performs two tests for randomness that provide information on the non-random variation due to trends, oscillation, mixtures and clustering.

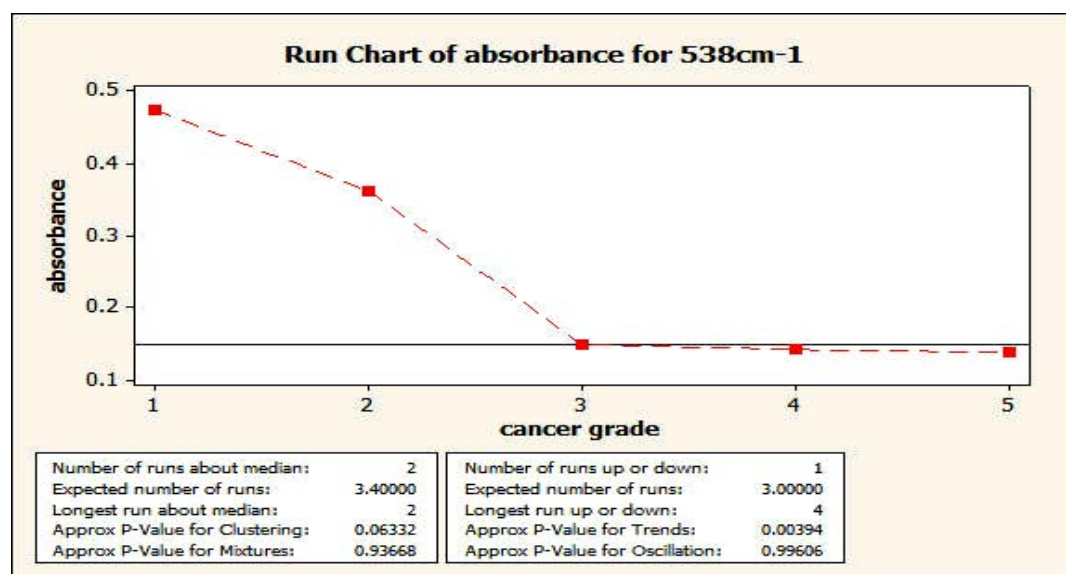


Figure-2(a): Run Chart Analysis for absorbance at 538 cm^{-1}

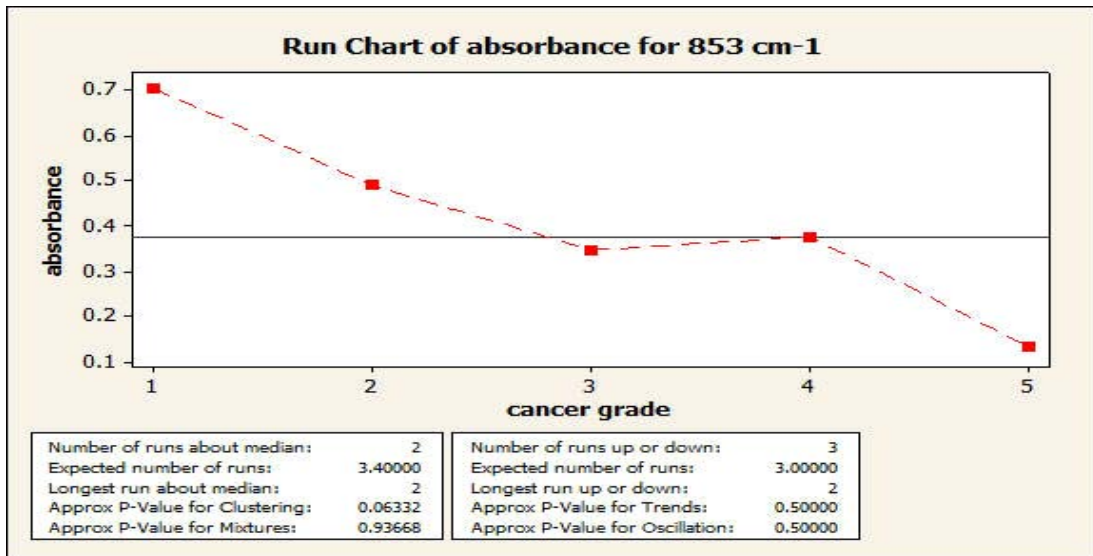


Figure-2(b): Run Chart Analysis for absorbance at 853 cm⁻¹

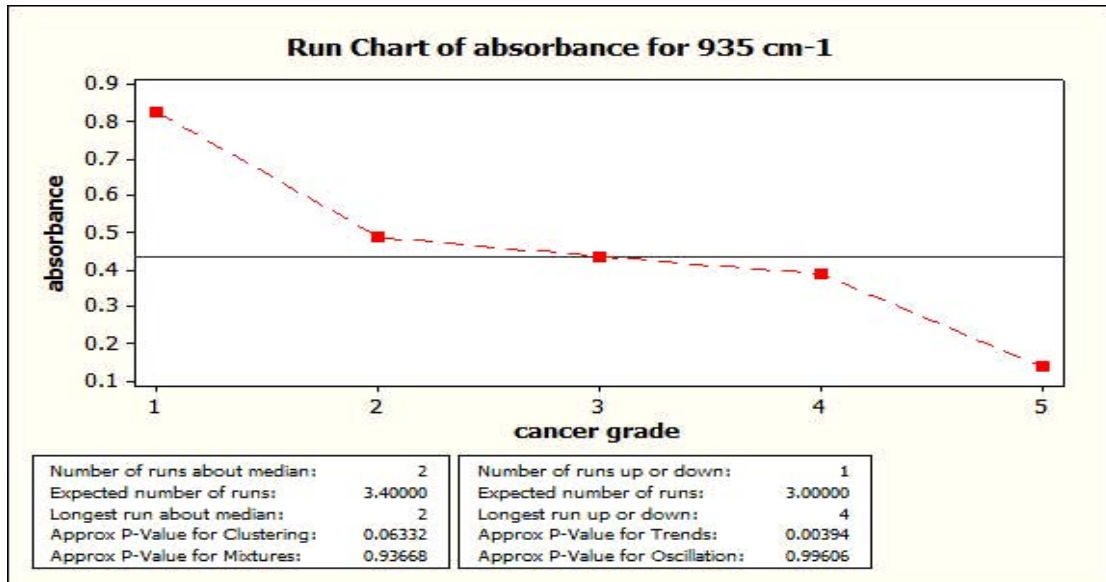


Figure-2(c): Run Chart Analysis for absorbance at 935 cm⁻¹

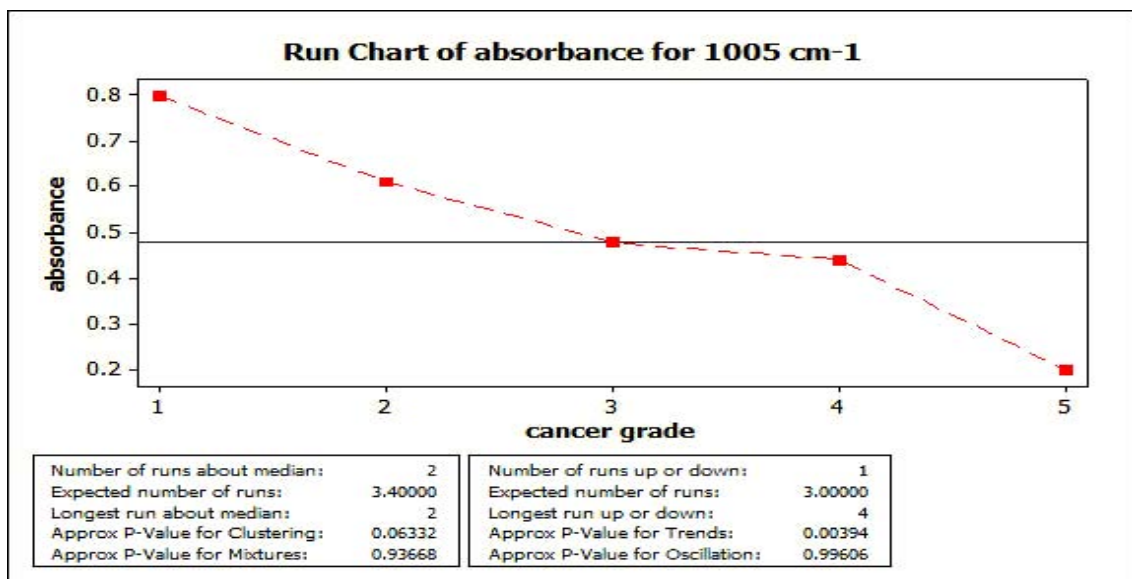


Figure-2(d): Run Chart Analysis for absorbance at 1005 cm⁻¹

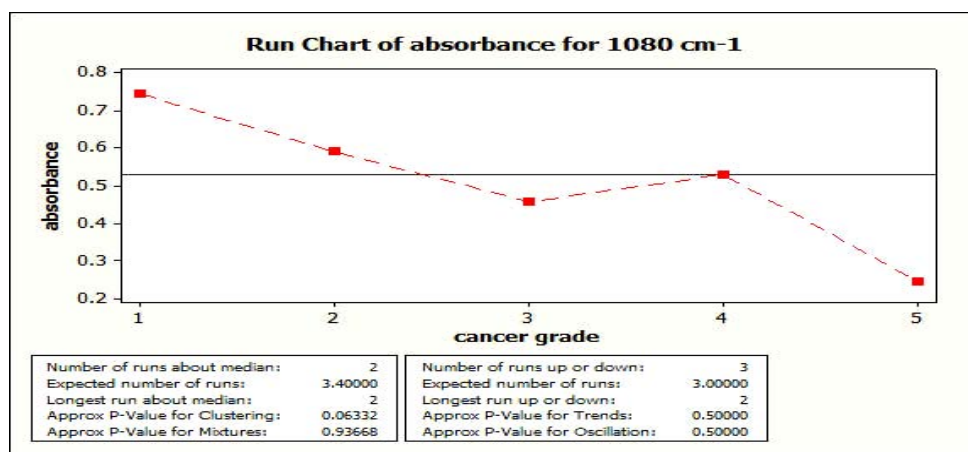


Figure-2(e): Run Chart Analysis for absorbance at 1080 cm⁻¹

TABLE 1: COMPARISON OF INTERNAL STANDARD RATIO AMONG FIVE CANCER GRADES.

Internal standard ratio	Normal	Hyperplasia	Fibro adenoma	Ductal carcinoma	Invasive ductal carcinoma
A _{538/853}	0.78333	0.77375	0.54000	0.31100	1.07250
A _{538/935}	0.57000	0.79375	0.49167	0.35111	1.77000
A _{538/1005}	0.540000	0.590000	0.418333	0.299000	0.634000
A _{538/1080}	0.543333	0.718750	0.461667	0.253000	0.562000
A _{853/935}	0.736667	0.998750	0.815000	0.998750	0.850000
A _{853/1005}	0.70333	0.77250	0.74167	0.83500	2.23600
A _{853/1080}	0.700000	0.857500	0.866667	0.771000	0.769000
A _{935/1005}	0.960000	0.796250	0.913333	0.878000	0.956000
A _{935/1080}	0.95667	0.81125	1.06667	0.86600	1.32800
A _{1005/1080}	1.08000	1.16222	1.11111	0.98000	1.80200

The Run chart of normal tissues, hyperplasia, fibro adenoma, ductal carcinoma and invasive ductal carcinoma breast tissues at 538 cm⁻¹, 853 cm⁻¹, 935 cm⁻¹, 1005 cm⁻¹ and 1080 cm⁻¹ are shown in figure-2(a), figure-2(b), figure-2(c), figure-2(d) and figure – 2(e) respectively.

CONCLUSION

The above results show that normal, hyperplasia, fibro adenoma, ductal carcinoma and invasive ductal carcinoma tissues have their own characteristic spectra and spectral parameters. Some notable differences exist between the spectra of these four kinds of breast cancer tissues in terms of spectral profiles, absorption values the absorption ratios of the major absorption bands. In carcinoma tissues a higher level of collagen was observed. These results which are in accordance with the histopathological observation such as nucleus condensation in carcinoma tissue collagen deposition in fibro adenoma tissue may show that the carcinogenesis process depend on the alterations of the composition of the connective tissues. Thus we have made use of the sensitivity of FTIR spectrum to study the biological changes happening in the cancerous tissues.

REFERENCES

- Oxford JT, Doege KJ, Morris NP. Alternative exon splicing within the amino-terminal nontriple-helical domain of the rat pro- α 1(XI) collagen chain generates multiple forms of the mRNA transcript which exhibit tissue-dependent variation. *J Biol Chem* 1995; 270: 9478–9485.
- Keene DR, Oxford JT, Morris NP. Ultrastructural localization of collagen types II, IX, and XI in the growth plate of human rib and fetal bovine epiphyseal cartilage: type XI collagen is restricted to thin fibrils. *J Histochem Cytochem* 1995; 43: 967–979.
- Gregory KE, Oxford JT, Chen Y, *et al.* Structural organization of distinct domains within the non-collagenous N-terminal region of collagen type XI. *J Biol Chem* 2000; 275: 11498–11506.
- Turashvili G, Bouchal J, Baumforth K, *et al.* Novel markers for differentiation of lobular and ductal invasive breast carcinomas by laser microdissection and microarray analysis. *BMC Cancer* 2007; 7:55.
- Feng Y, Sun B, Li X, *et al.* Differentially expressed genes between primary cancer and paired lymph

- node metastases predict clinical outcome of node-positive breast cancer patients. *Breast Cancer Res Treat* 2007;103:319–329.
6. Cechowska-Pasko M, Istrok;ka J, Wojtukiewicz MZ. Enhanced prolidase activity and decreased collagen content in breast cancer tissue. *Int J Exp Pathol* 2006; 87: 289–296.
 7. Fischer H, Stenling R, Rubio C, *et al.* Colorectal carcinogenesis is associated with stromal expression of COL11A1 and COL5A2. *Carcinogenesis* 2001; 22: 875–878.
 8. Chang H, Iizasa T, Shibuya K, *et al.* TI: increased expression of collagen XVIII and its prognostic value in nonsmall cell lung carcinoma. *Cancer* 2004; 100: 1665–1672.
 9. Banyard J, Bao L, Hofer MD, *et al.* Collagen XXIII expression is associated with prostate cancer recurrence and distant metastases. *Clinical Cancer Res* 2007; 13: 2634–2642.
 10. Burns-Cox N, Avery NC, Gingell JC, *et al.* Changes in collagen metabolism in prostate cancer: a host response that may alter progression. *J Urol* 2001; 166: 1698–1701.
 11. Wang KK, Liu N, Tadulovich N, *et al.* Novel candidate tumor marker genes for lung adenocarcinoma. *Oncogene* 2002; 21:7598–7604.
 12. Morris NP, Oxford JT, Gillian BM, *et al.* Developmentally regulated alternative splicing of the $\alpha 1(XI)$ collagen chain: spatial and temporal segregation of isoforms in the cartilage of fetal rat long bones. *J Histochem Cytochem* 2000; 48:725–741.
 13. Oxford JT, Doege KJ, Horton Jr WE, *et al.* Characterization of type II and type XI collagen synthesis by an immortalized rat chondrocyte cell line (IRC) having a low level of type II collagen mRNA expression. *Exp Cell Res* 1994; 213:28–36.
